Colloids and Surfaces A 533 (2017) 316–322

Contents lists available at ScienceDirect

Colloids and Surfaces A

journal homepage: www.elsevier.com/locate/colsurfa

Research Paper

Layered double hydroxide nanoparticles customization by polyelectrolyte adsorption: mechanism and effect on particle aggregation

Cecilia Vasti, Andrés Borgiallo, Carla E. Giacomelli, Ricardo Rojas*

INFIQC-CONICET, Departamento de Fisicoquímica, Facultad de Ciencias Químicas, Universidad Nacional de Córdoba, Ciudad Universitaria, 5000 Córdoba, Argentina

GRAPHICAL ABSTRACT

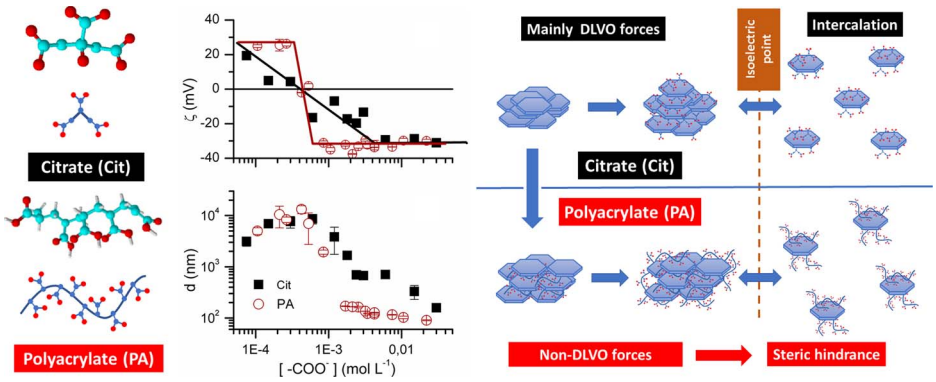

ARTICLE INFO

Keywords:
Inorganic/Organic hybrids
DLVO model
Zeta potential
Steric hindrance

ABSTRACT

Adsorption of polyelectrolytes (PEs) is a common strategy for stabilizing nanoparticles and customizing their properties. Although scarcely explored for layered double hydroxide nanoparticles (LDH-NPs), it can be used to increase their functionality in pharmaceutical and biomedical applications, among others. In this work, LDH-NPs intercalated with chloride, ibuprofen and ketoprofen were synthesized and modified with carboxylate containing PEs with different structures and physicochemical properties. The PEs adsorption mechanism on LDH-NPs and its effect on the aggregation of the obtained hybrids were studied by zeta potential and hydrodynamic diameter determinations on chloride intercalated LDH-NPs dispersions in the presence of polyacrylate (PA) at different concentrations. PA adsorption behavior was compared to that of citrate anion to contrast the adsorption mechanism of PEs and anions. Afterwards, the study was extended to other PEs (alginate and carbomer) as well as to drug intercalated LDH-NPs. PA adsorbed at the surface of LDH-NPs with high affinity: at low concentrations, PA was irreversibly adsorbed due to the positive structural charge of LDH-NPs and the flexible and negatively charged structure of PA. This high affinity caused a particle charge inversion, which results in negatively charged LDH-NPs stabilized by both electrostatic interactions and steric hindrance. Due to their structure, alginate and carbomer showed a lower affinity and, consequently, a lower capacity to produce LDH-NPs disaggregation. Finally, PEs adsorption allowed enhancing the disaggregation and modifying the interfacial properties of both ibuprofen and ketoprofen intercalated LDH-NPs producing only a small release of the drug loading.

* Corresponding author.
E-mail address: rrojas@fcq.unc.edu.ar (R. Rojas).

http://dx.doi.org/10.1016/j.colsurfa.2017.09.002
Received 30 June 2017; Received in revised form 1 September 2017; Accepted 1 September 2017
Available online 05 September 2017

1. Introduction

Adsorption of polymers and, particularly, polyelectrolytes (PEs), is a common strategy to prevent the aggregation of nanoparticles (NPs) and to customize their physicochemical and biological properties (particle charge, reactivity, chemical stability or toxicity) [1,2]. Several approaches have been developed to prepare NPs@PE hybrids [3,4], but physical adsorption is the most simple and it produces a fast and stable interaction between NPs and PEs [5,6]. PEs adsorption is determined by their own properties (molecular weight, structure, type of functional groups, concentration, etc.), the solution conditions (pH and ionic strength), and the nanoparticle characteristics (mainly their surface charge and size).

Layered double hydroxides (LDHs) are lamellar compounds whose structure can be described as brucite ($Mg(OH)_2$)-like layers with isomorphic substitution of divalent by trivalent metal ions. Consequently, they present a structural positive charge that allows the intercalation and exchange of anions, including drugs (anti-inflammatory, antibiotics and anticancer) and biomolecules (DNA, siRNA or proteins) [7,8]. LDHs can be synthesized as nanoparticles (LDH-NPs) with sizes between 50 and 200 nm by simple methods that involve separate nucleation and growth [9–11]. LDH-NPs aggregation is prevented by their highly positive zeta potential [12,13] but they aggregate in high ionic strength media or by the adsorption of anions that decrease the charge or increase the hydrophobicity of their surface [14–16].

Controlling LDH-NPs aggregation is of great importance for many of their applications and, particularly, for the biomedical and pharmaceutical ones. Thus, it is essential to determine their behavior in biological media or to customize their performance in liquid and semisolid pharmaceutical formulations. Although PEs adsorption is expected to be a versatile route to disaggregate LDH-NPs and increase their colloidal stability, there is scarce information about the subject [14,17,18]. LDH-NPs present a positive charge at pH lower than 12 [19] and, consequently, they present electrostatic interactions with anions and anionic PEs, as metal oxides do below their isoelectric point (iep) [1]. Polymers containing carboxylate, sulfonate or phosphonate groups are thus expected to adsorb on LDH-NPs [20].

Carboxylate containing PEs are extensively used for pharmaceutical applications and present a great variety of chain structures and physicochemical properties (Supplementary Material, Fig. S1). Thus, polyacrylate (PA) has been studied as component of drug delivery systems [21,22] and, due to its simple chemical formula, it is an ideal model to study the PEs adsorption mechanism on LDH-NPs. Carbomer (Carb) is used as gelling agent and presents mucoadhesive properties [23] that makes it appealing as drug carrier [24] for ophthalmic, nasal and oral formulations. Finally, Alginate (Alg) is used in cell encapsulation, tissue engineering and has also been proposed for the delivery of drugs and biomolecules [25–27]. Also, the inclusion of LDH-NPs in calcium alginate beads has been explored for the release of diclofenac [28].

In this work, LDH-NPs intercalated with chloride, ibuprofen and ketoprofen were synthesized and modified with three carboxylate containing PEs (PA, Carb and Alg). The PEs adsorption mechanism on LDH-NPs and its effect on the nanoparticles aggregation were studied by zeta potential and hydrodynamic diameter determinations with a simple system: chloride intercalated LDH-NPs dispersed in PA solutions at different concentrations. PA adsorption behavior was compared to that of citrate anion to contrast the adsorption mechanism of PEs and anions. Afterwards, the study was extended to other PEs (Alg and Carb) as well as to drug intercalated LDH-NPs.

2. Materials and methods

Pharmaceutical grade ibuprofen and ketoprofen (Parafarm®, Buenos Aires, Argentina), reagent grade metal chloride salts, citrate and sodium hydroxide (Baker, Anedra) and commercial sodium polyacrylate (Polacrin 40%w/w solution, Diransa, Argentina), sodium alginate (Laboratorios Montreal, Argentina) and carbomer (Carbomer 934P NF, BF Goodrich, USA) were used with no previous purification. All solutions were prepared with purified water (18MΩ Milli Q, Millipore System). Unless otherwise stated, all experiments were performed at room temperature.

2.1. Synthesis and characterization of LDH-NPs

LDH-NPs intercalated with either chloride (LDH-Cl-NPs), ibuprofen (LDH-Ibu-NPs) or ketoprofen (LDH-Ket-NPs) were synthesized by a method involving separate nucleation and aging steps [29]. Briefly, a 0.1 L solution containing the metal salts ($[Mg^{2+}] = 0.3\ mol\ L^{-1}$, $[Al^{3+}] = 0.1\ mol\ L^{-1}$) was quickly poured into a 0.1 L alkaline solution under vigorous stirring generated by an Ultraturrax T18 BASIC agitator at 25000 rpm. The alkaline solution contained the stochiometric amount of: a) NaOH to produce the complete precipitation of the metal ions ($[OH^-] = 0.8\ mol\ L^{-1}$); b) sodium salt of the interlayer anion ($A^- = Cl^-$, Ibu^- or Ket^-) to completely occupy all the exchange sites ($[A^-] = 0.1\ mol\ L^{-1}$). The prepared solid was immediately separated from the supernatants by centrifugation in 85 mL polycarbonate tubes, performed in an Allegra 21 Beckman-Coulter centrifugue, at 8000 rpm. Washing-centrifugation cycles were performed until turbidity was observed in the supernatants. The solid was then dispersed in water (0.2 L) and magnetically stirred for 24 h. Finally, the prepared dispersions were aged in hydrothermal conditions (4 h, 90 °C).

The hydrodynamic apparent diameter (d) and zeta potential (ζ) of the samples were determined using a Delsa Nano C instrument (Beckman Coulter). The measurements were performed in $1\ g\ L^{-1}$ dispersions of the corresponding samples, ultrasonically dispersed for 30 min. d values were determined from the autocorrelation function ($g^{(2)}$) using the cumulants method and the size distributions were evaluated by the CONTIN method, while electrophoretic mobilities were converted to ζ using the Smoluchowski equation. Scanning electron microscopy (SEM) images were obtained in a FE-SEM Σigma instrument on samples covered with a Cr layer. 0.05 mL of $0.1\ g\ L^{-1}$ dispersions of the samples were placed on the holder, which was afterwards dried at 50 °C.

Portions of the samples dispersions were lyophilized and the obtained powders were used to perform the structural characterization of the samples. Mg and Al contents were determined by atomic absorption spectrometry in a Varian AA240 instrument. The samples were dissolved in HNO_3 and afterwards diluted to meet the calibration range. Powder X-Ray diffraction (PXRD) patterns were recorded in a Phillips X'pert Pro instrument using a CuKα lamp (λ = 1.5408 Å) at 40 kV and 40 mA in step mode (0.05°, 1.2 s). Thermogravimetric and differential thermal analyses (TG/DTA) were carried out in a Shimadzu DTG 60 instrument in flowing air and at a heating rate of 10 °C/min. FT-IR spectra were measured in a Bruker IFS28 instrument using KBr pellets (1:100 sample:KBr ratio).

2.2. PEs adsorption on LDH-NPs

Due to the buffering capacity of LDH-NPs, experiments performed in pure water presents pH values between 10.0 and 10.2, but this pH range is of low relevance for LDH-NPs applications. Buffering the dispersion medium is a viable way to study the aggregation of LDH-NPs in more relevant pH conditions. Tris-HCl buffer (pH = 7.4; $[Tris] = 0.1\ mol\ L^{-1}$) was selected due to the low charge of its components (Tris, $HTris^+$ and Cl^-), which are consequently expected to present weak electrostatic interactions with LDH-NPs surface.

$1\ g\ L^{-1}$ LDH-Cl-NPs dispersions in $0.1\ mol\ L^{-1}$ Tris-HCl solutions (pH = 7.4) with increasing citrate (Cit), polyacrylate (PA), carbomer (Carb) and alginate (Alg) concentrations were prepared. These concentrations were converted to carboxylate groups concentration ($[COO^-]$, $mol\ L^{-1}$) taking into account the chemical formula of the

corresponding adsorbate. To obtain a deeper understanding of PA adsorption mechanism, the experiments with this PE were repeated at different LDH-Cl-NPs concentrations ([LDH] = 0.5, 1.0 and 2.0 g L^{-1}, the PA concentration being adjusted to maintain the same [COO^-]/[LDH] ratio) and [NaCl] (0, 0.1 and 0.3 mol L^{-1}). In all cases, the dispersions were equilibrated for 24 h under orbital shaking, and their *d* and ζ values afterwards determined as previously described. For PA and Cit series, PXRD patterns of the obtained solids were obtained the sedimentation stability of their dispersions was checked by taking images of the dispersions at different settling times.

Finally, PE adsorption on LDH-Cl-NPs, LDH-Ibu-NPs and LDH-Ket-NPs was studied in 1 g L^{-1} dispersions in water (to prevent anion exchange with chloride anions from Tris HCl buffer) and aqueous solutions of the corresponding adsorbates (Cit, PA, Carb or Alg; [COO^-] = 3 mmol L^{-1}). These dispersions were equilibrated for 24 h under orbital shaking, and their *d* and ζ values afterwards determined as previously described. Also, portions of LDH-Ibu-NPs and LDH-Ket-NPs dispersions were filtrated and the UV spectra of the supernatants were registered to determine the drug release (%D), which was calculated as:

$$\%D = \frac{[D]}{[D]_{max}}$$

where [D] was the drug concentration determined in the supernatants and $[D]_{max}$ is the drug concentration for a complete release of the drug cargo from the corresponding LDH-NPs.

3. Results and discussion

3.1. Synthesis and characterization of LDH-NPs

The size distributions of LDH-Cl-NPs, LDH-Ibu-NPs and LDH-Ket-NPs (Fig. 1) showed maxima at 80, 160 and 180 nm, respectively. These values were concordant with the size of the particles observed in the SEM images. Nevertheless, d values determined by the cumulants method (140 ± 50, 240 ± 70 nm and 300 ± 200 nm for LDH-Cl-NPs and LDH-Ibu-NPs, LDH-Ket-NPs, respectively) were larger while the polydispersity indexes were 0.14, 0.26 and 0.17. These results indicated the presence of particles of larger size doe to a partial aggregation of the particles.

Nevertheless, the LDH-NPs can be considered as mainly dissagregated, which was due to their large, positive ζ (=46 ± 1, 49 ± 1 and 40 ± 1 mV, for LDH-Cl-NPs and LDH-Ibu-NPs, LDH-Ket-NPs, respectively). The positive charging of LDH-NPs in aqueous media is due to the weak electrostatic interactions that bind these anions to the particle surface [12,13,16]. Therefore, the anions at the particle surface were detached from the particle surface in aqueous media, and the structural charge was not completely compensated, which generated a positive surface charge. Nevertheless, Ibu^- and Ket^- present a larger affinity for the surface of LDH-NPs due to the hydrophobic interactions between their hydrophobic tails. Adsorption of these drugs to the surface of LDH-NPs diminish its charge and increase their hydrophobicity [30,31], leading to aggregation. Consequently, minimizing their surface adsorption by repeatedly and thoroughly washing these samples before their aging was important to prepare well dispersed, nanometric LDH-NPs intercalated with Ket^- and Ibu^-.

Consequently, the exchange sites of LDH-NPs were not completely occupied by neither Ibu^- or Ket^- anions. Consequently, the chemical formulae of the samples (Table 1) pointed to an anion exchange capacity occupancy (% AEC) of 66 and 50% for LDH-Ibu-NPs and LDH-Ket-NPs, respectively. Despite the incomplete occupation of the exchange sites of drug intercalated LDH-NPs, the indexing of all PXRD patterns (Supplementary Material, Fig. S2A) led to cell parameters (*c* = 24.0 Å, 66.0 Å and 67.6 Å for LDH-Cl-NPs and LDH-Ibu-NPs, LDH-Ket-NPs, respectively; *a* = 3.06–3.08 Å in all cases) similar to those previously obtained for LDHs intercalated with the same anions [32,33]. Also, the FT-IR spectra (Supplementary Material, Fig. S2B) and the DTA/TGA curves (Supplementary material, Fig. S2C) were similar to those previously determined for LDHs intercalated with the same anions [30].

The characterization of ζ and d dependence with ionic strength was performed both in water and Tris-HCl buffer (Supplementary Material, Fig. S3). As expected, LDH-Cl-NPs showed decreasing ζ and increasing d with increasing ionic strength, showing d values above 1 μm in Tris buffer and/or [NaCl] above 0.01 mol L^{-1} due to the decrease of the electrostatic repulsions between LDH-Cl-NPs.

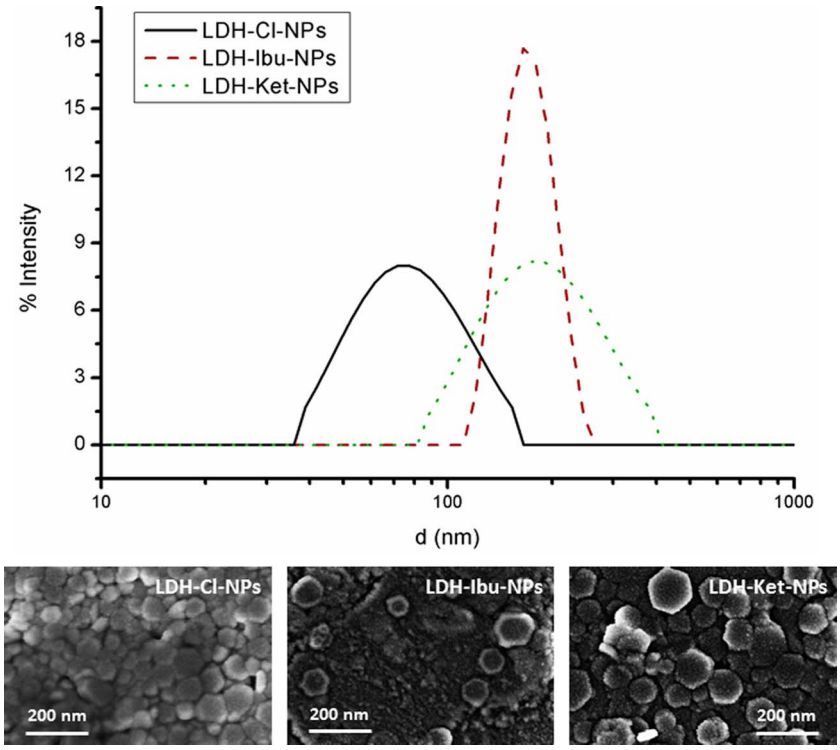

Fig. 1. Intensity size distribution (above) and SEM images (below) of LDH-NPs samples intercalated with chloride (LDH-Cl-NPs), ibuprofen (LDH-Ibu-NPs) and ketoprofen (LDH-Ket-NPs).

Table 1
Elemental analysis and chemical formulae of LDH samples.

Sample	%Mg	%Al	%C	% H_2O[a]	Chemical Formula
LDH−Cl-NPs	22.8	9.0	N/A	13.5	$Mg_{0.74}Al_{0.26}(OH)_2Cl_{0.24}{\cdot}0.58H_2O$
LDH-Ibu-NPs	17.0	6.1	23.9	14.2	$Mg_{0.76}Al_{0.24}(OH)_2Ibu_{0.16}Cl_{0.08}{\cdot}0.85H_2O$
LDH-Ket-NPs	17.2	6.8	22.3	12.0	$Mg_{0.74}Al_{0.26}(OH)_2Ket_{0.13}Cl_{0.12}{\cdot}0.68H_2O$

[a] Obtained from the first weight loss of the thermogravimetric analysis curve.

3.2. Polymer adsorption on LDH-NPs

d and ζ vs. [−COO^-] curves were used to explore and compare Cit and PA adsorption on LDH-NPs (Fig. 2A and B). A schematic representation of the mechanism of Cit and PA adsorption on LDH-NPs is also provided (Fig. 2C) for further reference. Cit anion present three carboxylate groups at pH = 7.4 and it was expected to present strong electrostatic interactions with LDH-Cl-NPs. For Cit adsorption, ζ decreased as [−COO^-] increased until an isoelectric point (iep) was reached at 5 10^{-4} mol L^{-1} approximately, which corresponded to ca. 15% AEC. The continuous ζ diminution and the low [−COO^-] of the iep indicated that Cit was preferably adsorbed on the LDH-NPs surface (Fig. 2A), similarly to that observed for dodecylsulfate uptake by chloride intercalated LDHs [34]. Once the surface became negatively charged, Cit anions adsorption was increasingly hindered by electrostatic repulsions. Therefore, Cit anions increasingly located between the layers of LDH-Cl-NPs and a ζ plateau was reached at ca. [−COO^-] = 4 10^{-3} mol L^{-1}, corresponding to near 120% AEC. The intercalation of Cit anions reflected in the progressive widening and intensity diminution of the (0 0 L) peaks of chloride- intercalated samples and the presence of a peak at [−COO^-] = 4 10^{3} mol L^{-1}, corresponding to a interplanar distance of 12 Å (Supplementary Material, Fig. S4). This interplanar distance was similar to that found for citrate-intercalated LDHs [35]. Regarding the effect of Cit incorporation to the particle size, LDH-Cl-NPs maintained their high aggregation before the iep was reached and d values above 1 10^{3} nm were obtained. At larger [−COO^-] values, the aggregation progressively diminished due to increasing repulsive electrostatic forces between the particles and *d* values reached near 200 nm at the larger [−COO^-] value. The effects in the aggregation of LDH-Cl-NPs were similar to those observed with trivalent inorganic anions, such as phosphate [16].

In contrast with Cit anion, PA is a PE with a linear structure based on acrylate (−CH_2−CH−COO^-) monomers (Supplementary Material, Fig. S1). Although it is a weakly acid PE, it presents mainly carboxylate groups at pH = 7.4 [36] and, consequently, it was expected to strongly adsorb to the oppositely charged surface of LDH-Cl-NPs. ζ (Fig. 2A) showed a negligible change at [−COO^-] below 3 10^{-4} mol L^{-1}, but it abruptly diminished at larger [-COO^-] values to reach an iep at a [−COO^-] value close to that of Cit. This diminution continued until a plateau was reached, at a [−COO^-] value lower than that of Cit anion ([−COO^-] = 6–7 10^{-4} mol L^{-1}, corresponding to 20–25% of the AEC). The low [−COO^-] of the plateau onset was related to the limited capacity of PA chains to penetrate in the interlayer space of LDH-Cl-NPs. These results indicated that PA was quantitatively adsorbed to the surface of LDH-Cl-NPs at [−COO^-] values lower than the iep, which is the general behavior for PEs adsorption on oppositely charged surfaces [37], which is considered an irreversible process. Only after the iep, electrostatic repulsions increase and a ζ plateau was reached without significant PA intercalation. The PXRD patterns (Supplementary Material, Fig. S4) showed a widening of the peaks corresponding to the chloride intercalated phase, but, contrarily to the Cit-modified LDH-Cl-NPs, no additional peak was registered even at the larger [COO^-] value.

The effect of PA adsorption on the aggregation of LDH-NPs was explained by both DLVO and non-DLVO interactions. Thus, the aggregation of PA-modified LDH-Cl-NPs was maintained at concentrations below the iep due to the low electrostatic repulsions. Nevertheless, it has been proposed that bridging interactions are concurrent for systems such as metal oxide particles [5]. This mechanism is based on the heterogeneus disposition PEs on the surface of NPs at low surface coverages, which leads to the presence of oppositely charged patches due to coated and uncoated areas. These patches interact with oppositely charged patches of neighboring particles, leading to reinforced aggregation. Above the iep, the aggregation decreased greatly, reaching values even lower to that of LDH-Cl-NPs dispersions in water. In this section, the PA layer became more homogenous and swollen, as a portion of the chains are not directly attached to the surface but interacting with the aqueous side of the interface. This swollen PE layer led to steric interactions [38,39] that prevented, together with electrostatic repulsions, the aggregation of LDH-Cl-NPs.

The effect of PE adsorption on the aggregation of LDH-Cl-NPs reflected in the stability of the dispersions against sedimentation

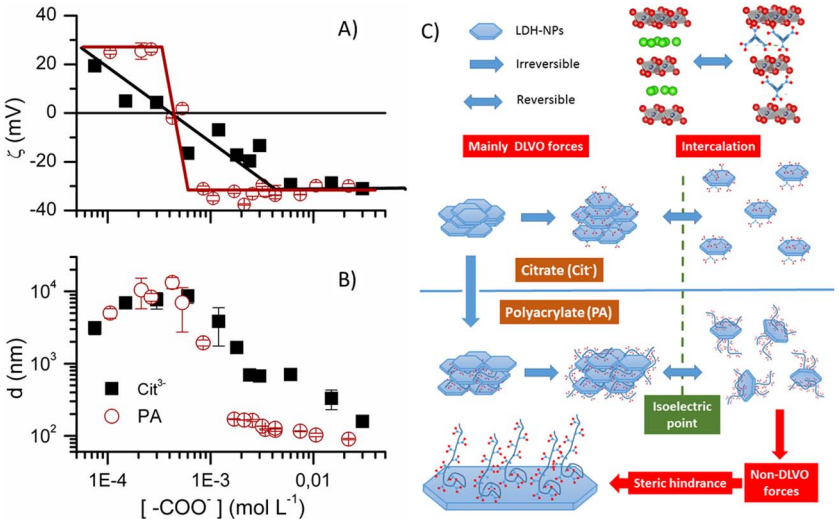

Fig. 2. Zeta potential (ζ, A) and hydrodynamic diameter (*d*, B) vs. carboxylate groups concentration ([-COO^-]) provided by Cit and PA. The experiments were performed in LDH-Cl-NPs dispersions in Tris-HCl buffer (0.1 mol L^{-1}, pH = 7.4) with increasing Cit and PA concentrations. Schematic representation of the proposed adsorption mechanism as well as its effect on LDH-Cl-NPs aggregation (C).

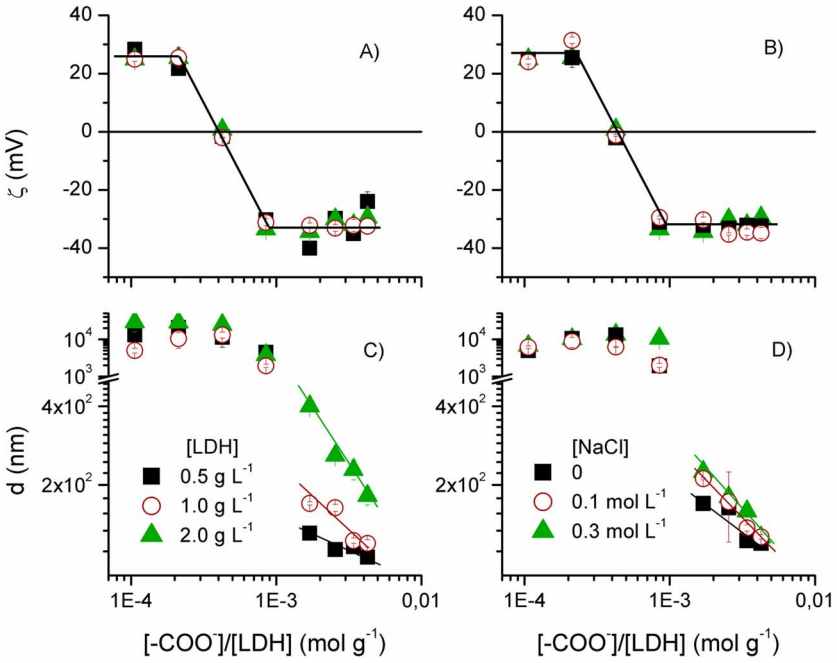

Fig. 3. Zeta potential (ζ, A and B) and hydrodynamic diameter (*d*, C and D) vs. the ratio between PA (expressed as carboxylate groups concentration provided by this PE, ([-COO^-]) and LDH-Cl-NPs concentrations ([LDH]) of LDH-Cl-NPs dispersions in Tris-HCl buffer 0.1 mol L^{-1}, pH = 7.4) with increasing PA concentration. The experiments were performed at fixed NaCl concentration ([NaCl] = 0) and different LDH-Cl-NPs concentration ([LDH] = 0.5, 1.0 and 2.0 g L^{-1}; Fig. 3A and C); and also at fixed [LDH] = 0.1 g L^{-1} and different [NaCl] (=0, 0.1 mol L^{-1} and 0.3 mol L^{-1}, Fig. 3B and D).

(Supplementary Material, Fig. S5). LDH-Cl-NPs showed increasing sedimentation stability with increasing [$-COO^-$] for both Cit and PA, but the stabilizing effect of PA was obtained at lower [$-COO^-$]. Also, PA containing dispersions presented, at t = 0, lower turbidity than the Cit containing ones for all [$-COO^-$].

The study of PA adsorption on LDH-Cl-NPs was complemented with ζ and *d* vs [-COO^-] curves at different LDH-Cl-NPs ([LDH]) and NaCl ([NaCl]) concentrations (Fig. 3). The ζ vs [-COO^-]/[LDH] curves (Fig. 3A and B) were independent of both [LDH] and [NaCl]. The independence of ζ curves with the sorbent concentration is characteristic of irreversible, quantitative adsorption, which completely removed the adsorbate from solution [38,40]. In this case, the adsorbed amount is determined exclusively by the amount of sorption sites available, which is directly proportional to the sorbent concentration ([LDH] in this work). Contrarily, when the adsorption is not quantitative and the adsorbate is distributed between the solution and the particles, ζ vs [$-COO^-$]/[LDH] would be determined not only by the number of sites available for adsorption, but also by the affinity of the adsorbate for these sites.

On the other hand, the negligible effect of ionic strength on ζ values was not concordant with that found for adsorption of highly-charged polymers onto latex NPs [5]. For these systems, the beginning of the ζ plateau is moved to larger PE concentration with increasing ionic strength, which was assigned to a diminution of electrostatic repulsions between the PE chains. This effect is significant because the adsorption sites for PEs is relatively low. However, in the case of LDH-Cl-NPs, PA adsorption was determined by their large surface concentration of adsorption sites and the PE adsorption capacity increase due to increasing ionic strength was negligible in comparison.

The *d* vs [$-COO^-$]/[LDH] curves (Fig. 3C and D) showed up to [$-COO^-$]/[LDH] = 1 10^{-3} mol g^{-1} a stage of high agglomeration that presented d values above 1 μm, This region included the first point of the plateau of the ζ vs. [$-COO^-$]/[LDH] curves, which confirmed that the main driving force for the disaggregation of LDH-Cl-NPs was not electrostatic repulsions, but steric hindrance. At larger [$-COO^-$]/[LDH] a second region was defined by *d* values lower than 500 nm that decreased with increasing [LDH] and [$-COO^-$]/[LDH]It is a general behavior of colloidal particles that the effect of particle concentration on aggregation is negligible until a narrow concentration range where a large aggregation increase is produced [39]. This concentration range is usually designed as critical coagulation concentration (CCC). For LDH-Cl-NPs, PA adsorption produced a CCC shifting to higher concentrations, but d values increased as [LDH] increases, approaching to the CCC. Moreover, the d values diminution indicated that additional PE adsorption was produced at the plateau, increasing the thickness of the PE layer and, consequently, the steric effects. The convergence of the curves was consequently explained by this effect which produced a CCC shifting to higher particle concentrations, diminishing the effect of [LDH]. On the other hand, the dependence of *d* values with [NaCl] was weaker, which confirmed once again that the incidence of electrostatic repulsions in the stabilization of LDH-Cl-NPs was lower than that of steric hindrance.

The PEs-NPs interaction is highly determined by the structure of the PEs [37]. To study this effect, ζ and d vs. [$-COO^-$] curves were measured for two additional PEs: Carb and Alg (Fig. 4A and B). A schematic representation of the proposed mechanism of Carb and Alg adsorption on LDH-NPs is also provided (Fig. 4C) for further reference. Carb showed a subtler ζ diminution with increasing [$-COO^-$] than PA (Fig. 2A): the iep was displaced to [$-COO^-$] = 1 10^{-3} mol L^{-1} approximately, while the ζ plateau was reached at [$-COO^-$] = $3{\cdot}10^{-3}$ mol L^{-1}. Also, disaggregation of LDH-Cl-NPs was produced at larger [$-COO^-$] values, reaching d values below 1 μm only at [$-COO^-$] = 1 10^{-2} mol L^{-1}. On the other hand, ζ diminution was produced at lower concentrations for Alg than for PA: the iep was reached at [$-COO^-$] = 1.5 10^{-4} mol L^{-1}, while the onset of the ζ plateau was placed at [$-COO^-$] = 4 10^{-4} mol L^{-1}. Nevertheless, the aggregation diminution started at [$-COO^-$] values similar to that of PA, but Alg adsorption produced *d* values around 500 nm.

The structure of these PEs (Supplementary Material, Fig. S1) caused their different adsorption behavior. Carb is a crosslinked derivative of polyacrylates and, due to its more rigid structure, many of its carboxylate groups were not able to interact with LDH-Cl-NPs surface or are compensated in the bulk of the PE. Consequently, they present a weaker interaction with LDHs and, contrarily to PA, Carb was not quantitatively adsorbed to the surface of LDH-Cl-NPs. As a consequence, the ζ diminution was gentler and the iep (as well as the LDH-Cl-NPs disaggregation effect) is displaced to larger [$-COO^-$] values. On the other hand, Alg is a block copolymer with a linear structure that combines β-D-mannunorate and α-L-guluronate in different ratio depending on their source of extraction. Due to its linear structure, Alg presented higher affinity for the LDH-Cl-NPs aggregates than Carb, but it displayed a

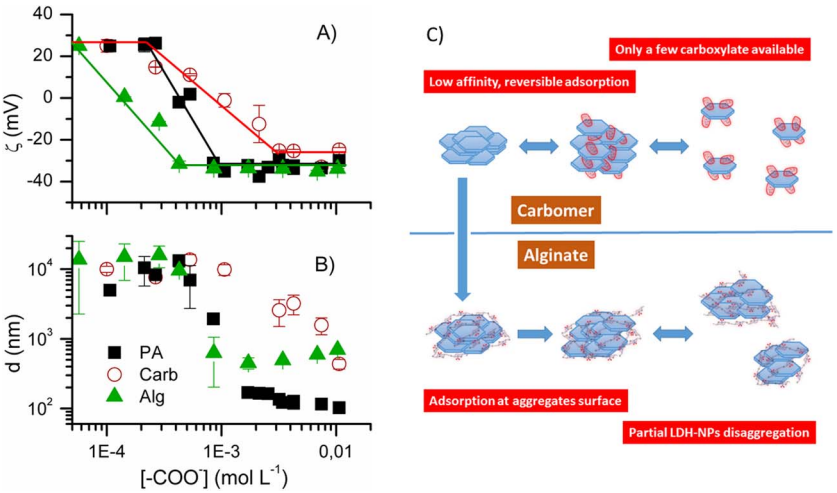

Fig. 4. Zeta potential (ζ, A) and hydrodynamic diameter (*d*, B) vs. carboxylate groups concentration ([-COO⁻]) provided by PA, Carb and Alg of LDH-Cl-NPs particles in Tris-HCl buffer with increasing PA, Carb and Alg concentrations. Schematic representation of the adsorption mechanism of Carbomer and Alginate as well as its effect in LDH-Cl-NPs aggregation (C).

lower affinity than PA due to their larger charge/mass ratio of the latter. Consequently, Alg was not able to penetrate the LDH-Cl-NPs aggregates at low concentrations. Instead, Alg coated the aggregates, which explained the ζ diminution at lower [−COO⁻] than for PA. On the other hand, the disaggregation begins at [−COO⁻] values similar to that of PA but, due to its lower affinity, Alg did not produce d values below 500 nm.

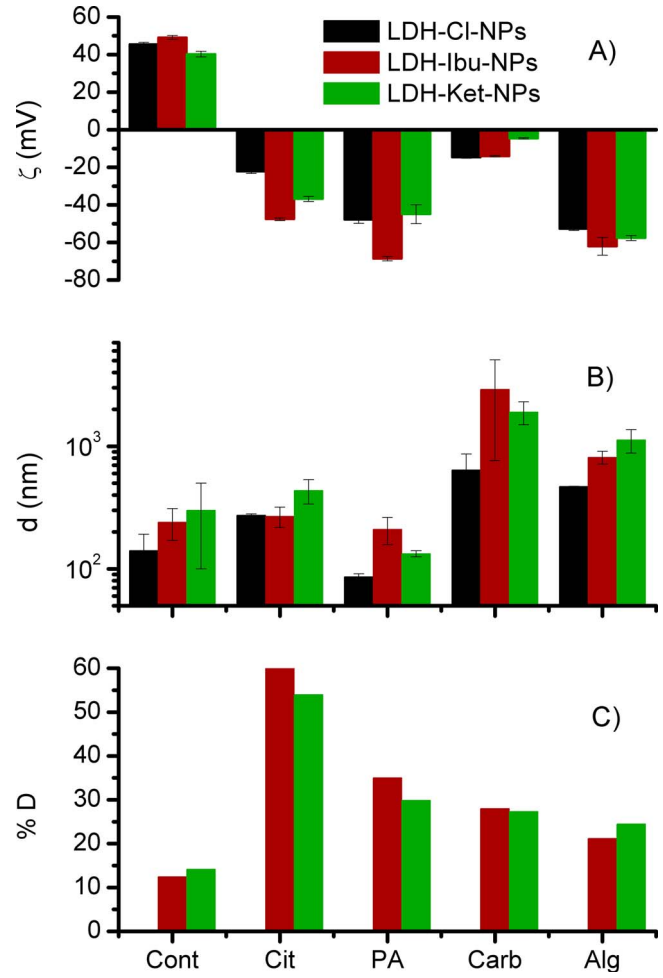

Fig. 5. Zeta potential (ζ, A), hydrodynamic diameter (d, B) and drug release percentage (% D, C) of LDH-Cl-NPs (1 g L^{-1}) dispersions in water (used as a control, Cont) and in 3 10^{-3} mol L^{-1} Cit, PA, Carb and Alg solutions in water.

Finally, the effect of PE adsorption on the size, zeta potential and drug release of Ibu^- and Ket^- containing LDH-NPs was assessed (Fig. 5, where LDH-Cl-NPs data are also included to allow comparison). To determine effect of PE adsorption on drug release from LDH-Ibu-NPs and LDH-Ket-NPs, the experiments were performed in water, as anion exchange would have been produced with Cl^- anions of Tris HCl buffer. Nevertheless, the effects on d and ζ upon PE adsorption were similar to that observed for LDH-Cl-NPs in Tris HCl: ζ was reversed in all cases and the disaggregation capacity decreased in the order PA > Cit > Alg ≈ Carb. Thus, PA was able to completely disaggregate all LDH-NPs, obtaining d values (86 ± 5, 210 ± 50 nm and 130 ± 10 for LDH-Cl-NPs, LDH-Ibu-NPs and LDH-Ket-NPs, respectively) lower than that of the particles in water. On the other hand, Carb and Alg produced only a partial disaggregation in all cases. Both d and ζ values were independent of the intercalated anion, which indicated that the charge and size of LDH-NPs was mainly determined by the adsorpted PEs. Moreover, PEs adsorption produced a low drug release from LDH-Ibu-NPs and LDH-Ket-NPs, less than 40% in all cases. On the other hand, Cit coated LDH-Ibu-NPs and LDH-Ket-NPs presented the higher drug release (% D > 50%) due to its capacity to intercalate between the layers of LDH-NPs. Both LDH-Ibu-NPs and LDH-Ket-NPs showed% D values for PA than for Carb and Alg, which suggested that PA had a slightly larger capacity than the other PEs to intercalate between the LDH-NPs layers due to its linear, simple structure.

4. Conclusions

LDH-NPs intercalated with chloride, ibuprofen and ketoprofen with diameter below 200 nm were synthesized. They were stabilized by electrostatic repulsions due to their high particle charge, but agglomerated with increasing ionic strength. Polyacrylate (PA) adsorbed at their surface with great affinity: at low concentrations, PA adsorbed irreversibly to the surface of LDH-NPs due to the large positive surface charge of LDH-NPs and the flexible and charged structure of linear PEs. This high affinity results in negatively charged LDH-NPs stabilized by both electrostatic interactions and steric hindrance. The behavior of other PEs, such as carbomer and alginate was affected by their structure. Although both adsorbed on LDH-NPs, the crosslinked, rigid structure of the former and the lower charge density of the latter led to a lower capacity of LDH-NPs disaggregation than PA. PEs interaction with LDH-NPs determined the surface properties of both chloride and drug intercalated LDH-NPs while the main portion of the interlayer anion remains attached between the layers. This is then a promising strategy to obtain drug carriers with tunable particle size and interfacial properties, as well as increased functionality.

Acknowledgements

Economic supports by SeCyT-UNC, project number 05/C585, FONCyT, project PICT 12/0634, and CONICET, PIP 11220120100575, are gratefully acknowledged. CV acknowledge grants of CONICET. SEM images were obtained at the Laboratorio de Microscopía Electrónica y Análisis por Rayos X (LAMARX).

Appendix A. Supplementary data

Supplementary data associated with this article can be found, in the online version, at http://dx.doi.org/10.1016/j.colsurfa.2017.09.002.

References

[1] P.L. Golas, S. Louie, G.V. Lowry, K. Matyjaszewski, R.D. Tilton, Comparative study of polymeric stabilizers for magnetite nanoparticles using ATRP, Langmuir 26 (2010) 16890–16900, http://dx.doi.org/10.1021/la103098q.
[2] I. Szilagyi, A. Sadeghpour, M. Borkovec, Destabilization of colloidal suspensions by multivalent ions and polyelectrolytes: from screening to overcharging, Langmuir 28 (2012) 6211–6215, http://dx.doi.org/10.1021/la300542y.
[3] S. Laurent, D. Forge, M. Port, A. Roch, C. Robic, L. Vander Elst, et al., Magnetic iron oxide nanoparticles: synthesis, stabilization, vectorization, physicochemical characterizations and biological applications, Chem. Rev. 108 (2008) 2064–2110, http://dx.doi.org/10.1021/cr068445e.
[4] A.K. Gupta, M. Gupta, Synthesis and surface engineering of iron oxide nanoparticles for biomedical applications, Biomaterials 26 (2005) 3995–4021, http://dx.doi.org/10.1016/j.biomaterials.2004.10.012.
[5] A. Tiraferri, M. Borkovec, Probing effects of polymer adsorption in colloidal particle suspensions by light scattering as relevant for the aquatic environment: an overview, Sci. Total Environ. 535 (2015) 131–140, http://dx.doi.org/10.1016/j.scitotenv.2014.11.063.
[6] H. Li, M.J. Henderson, K. Wang, X. Tuo, Y. Leng, K. Xiong, et al., Colloidal assembly of magnetic nanoparticles and polyelectrolytes by arrested electrostatic interaction, Colloids Surf. A Physicochem. Eng. Asp. 514 (2017) 107–116, http://dx.doi.org/10.1016/j.colsurfa.2016.11.049.
[7] Y. Kuthati, R.K. Kankala, C. Lee, Layered double hydroxide nanoparticles for biomedical applications: current status and recent prospects, Appl. Clay Sci. 112–113 (2015) 100–116, http://dx.doi.org/10.1016/j.clay.2015.04.018.
[8] V. Rives, M. del Arco, C. Martín, Intercalation of drugs in layered double hydroxides and their controlled release: a review, Appl. Clay Sci. 88–89 (2014) 239–269, http://dx.doi.org/10.1016/j.clay.2013.12.002.
[9] Y. Zhang, H. Li, N. Du, R. Zhang, W. Hou, Large-scale aqueous synthesis of layered double hydroxide single-layer nanosheets, Colloids Surf. A Physicochem. Eng. Asp. 501 (2016) 49–54, http://dx.doi.org/10.1016/j.colsurfa.2016.04.046.
[10] R. Rojas, D. Aristizabal Bedoya, C. Vasti, C.E. Giacomelli, LDH nanoparticles: synthesis, size control and applications in nanomedicine, in: I.T. Sherman (Ed.), Layer. Double Hydroxides, Nova Press, New York, 2015, pp. 101–120.
[11] C. Vasti, V. Pfaffen, E. Ambroggio, M.R. Galiano, R. Rojas, C.E. Giacomelli, A systematic approach to the synthesis of LDH nanoparticles by response surface methodology, Appl. Clay Sci. 137 (2017) 151–159, http://dx.doi.org/10.1016/j.clay.2016.12.023.
[12] R. Rojas, C. Barriga, C.P. De Pauli, M.J. Avena, Influence of carbonate intercalation in the surface-charging behavior of Zn-Cr layered double hydroxides, Mater. Chem. Phys. 119 (2010) 303–308, http://dx.doi.org/10.1016/j.matchemphys.2009.09.001.
[13] Z.P. Xu, Y. Jin, S. Liu, Z.P. Hao, G.Q.M. Lu, Surface charging of layered double hydroxides during dynamic interactions of anions at the interfaces, J. Colloid Interface Sci. 326 (2008) 522–529, http://dx.doi.org/10.1016/j.jcis.2008.06.062.
[14] C. Vasti, D.A. Bedoya, R. Rojas, C.E. Giacomelli, Effect of the protein corona on the colloidal stability and reactivity of LDH-based nanocarriers, J. Mater. Chem. B 4 (2016) 2008–2016, http://dx.doi.org/10.1039/C5TB02698A.
[15] M. Pavlovic, P. Rouster, T. Oncsik, I. Szilagyi, Tuning colloidal stability of layered double hydroxides: from monovalent ions to polyelectrolytes, ChemPlusChem 82 (2017) 121–131, http://dx.doi.org/10.1002/cplu.201600295.
[16] M. Pavlovic, R. Huber, M. Adok-Sipiczki, C. Nardin, I. Szilagyi, Ion specific effects on the stability of layered double hydroxide colloids, Soft Matter 12 (2016) 4024–4033, http://dx.doi.org/10.1039/C5SM03023D.
[17] H. Zuo, Z. Gu, H. Cooper, Z.P. Xu, Crosslinking to enhance colloidal stability and redispersity of layered double hydroxide nanoparticles, J. Colloid Interface Sci. 459 (2015) 10–16, http://dx.doi.org/10.1016/j.jcis.2015.07.063.
[18] M. Pavlovic, M. Adok-Sipiczki, C. Nardin, S. Pearson, E. Bourgeat-Lami, V. Prevot, et al., Effect of MacroRAFT copolymer adsorption on the colloidal stability of layered double hydroxide nanoparticles, Langmuir 31 (2015) 12609–12617, http://dx.doi.org/10.1021/acs.langmuir.5b03372.
[19] R. Rojas Delgado, M. Arandigoyen Vidaurre, C.P. De Pauli, M.A. Ulibarri, M.J. Avena, Surface-charging behavior of Zn-Cr layered double hydroxide, J. Colloid Interface Sci. 280 (2004) 431–441, http://dx.doi.org/10.1016/j.jcis.2004.08.045.
[20] D. Li, X. Xu, J. Xu, W. Hou, Poly(ethylene glycol) haired layered double hydroxides as biocompatible nanovehicles: morphology and dispersity study, Colloids Surf. A 384 (2011) 585–591, http://dx.doi.org/10.1016/j.colsurfa.2011.05.012.
[21] J.C. Garay-Jimenez, E. Turos, A convenient method to prepare emulsified polyacrylate nanoparticles from powders [corrected] for drug delivery applications, Bioorg. Med. Chem. Lett. 21 (2011) 4589–4591, http://dx.doi.org/10.1016/j.bmcl.2011.05.104.
[22] M. Khajeh, S. Laurent, K. Dastafkan, Nanoadsorbents: classification preparation, and applications (with emphasis on aqueous media), Chem. Rev. 113 (2013) 7728–7768.
[23] A.K. Singla, M. Chawla, A. Singh, Potential applications of carbomer in oral mucoadhesive controlled drug delivery system: a review, Drug Dev. Ind. Pharm. 26 (2000) 913–924, http://dx.doi.org/10.1081/DDC-100101318.
[24] A.F. Jimenez-Kairuz, D.A. Allemandi, R.H. Manzo, The improvement of aqueous chemical stability of a model basic drug by ion pairing with acid groups of polyelectrolytes, Int. J. Pharm. 269 (2004) 149–156, http://dx.doi.org/10.1016/j.ijpharm.2003.09.008.
[25] K.Y. Lee, D.J. Mooney, Alginate: properties and biomedical applications, Prog. Polym. Sci. 37 (2012) 106–126, http://dx.doi.org/10.1016/j.progpolymsci.2011.06.003.
[26] J.A. Rowley, G. Madlambayan, D.J. Mooney, Alginate hydrogels as synthetic extracellular matrix materials, Biomaterials 20 (1999) 45–53, http://dx.doi.org/10.1016/S0142-9612(98)00107-0.
[27] W.R. Gombotz, S.F. Wee, Protein release from alginate matrices, Adv. Drug Deliv. Rev. 64 (2012) 194–205, http://dx.doi.org/10.1016/j.addr.2012.09.007.
[28] J.P. Zhang, Q. Wang, X.L. Xie, X. Li, A.Q. Wang, Preparation and swelling properties of pH-sensitive sodium alginate/layered double hydroxides hybrid beads for controlled release of diclofenac sodium, J. Biomed. Mater. Res. - Part B Appl. Biomater. 92 (2010) 205–214, http://dx.doi.org/10.1002/jbm.b.31507.
[29] D.A. Bedoya, C. Vasti, R. Rojas, C.E. Giacomelli, Risedronate functionalized layered double hydroxides nanoparticles with bone targeting capabilities, Appl. Clay Sci. 141 (2017) 257–264, http://dx.doi.org/10.1016/j.clay.2017.03.001.
[30] R. Rojas, A.F. Jimenez-Kairuz, R.H. Manzo, C.E. Giacomelli, Release kinetics from LDH-drug hybrids: effect of layers stacking and drug solubility and polarity, Colloids Surf. A Physicochem. Eng. Asp. 463 (2014) 37–43, http://dx.doi.org/10.1016/j.colsurfa.2014.09.031.
[31] R. Rojas, Y.G. Linck, S.L. Cuffini, G.a. Monti, C.E. Giacomelli, Structural and physicochemical aspects of drug release from layered double hydroxides and layered hydroxide salts, Appl. Clay Sci. 109–110 (2015) 119–126, http://dx.doi.org/10.1016/j.clay.2015.02.030.
[32] M.S. San Román, M.J. Holgado, B. Salinas, V. Rives, Characterisation of Diclofenac, Ketoprofen or Chloramphenicol Succinate encapsulated in layered double hydroxides with the hydrotalcite-type structure, Appl. Clay Sci. 55 (2012) 158–163, http://dx.doi.org/10.1016/j.clay.2011.11.010.
[33] R. Rojas, M.C. Palena, A.F. Jimenez-Kairuz, R.H. Manzo, C.E. Giacomelli, Modeling drug release from a layered double hydroxide-ibuprofen complex, Appl. Clay Sci. 62–63 (2012) 15–20, http://dx.doi.org/10.1016/j.clay.2012.04.004.
[34] R. Rojas, F. Bruna, C.P. de Pauli, Ulibarri M.Á, C.E. Giacomelli, The effect of interlayer anion on the reactivity of Mg-Al layered double hydroxides: improving and extending the customization capacity of anionic clays, J. Colloid Interface Sci. 359 (2011) 136–141, http://dx.doi.org/10.1016/j.jcis.2011.03.056.
[35] M. Meyn, K. Beneke, G. Lagaly, Anion-Exchange reactions of layered double hydroxides, Inorg. Chem. 29 (1990) 5201–5207, http://dx.doi.org/10.1021/ic00351a013.
[36] A. Hajdú, M. Szekeres, I.Y. Tóth, R.A. Bauer, J. Mihály, I. Zupkó, et al., Enhanced stability of polyacrylate-coated magnetite nanoparticles in biorelevant media, Colloids Surf. B Biointerfaces 94 (2012) 242–249, http://dx.doi.org/10.1016/j.colsurfb.2012.01.042.
[37] I. Szilagyi, G. Trefalt, A. Tiraferri, P. Maroni, M. Borkovec, Polyelectrolyte adsorption, interparticle forces, and colloidal aggregation, Soft Matter 10 (2014) 2479–2502, http://dx.doi.org/10.1039/c3sm52132j.
[38] J. Hierrezuelo, A. Vaccaro, M. Borkovec, Stability of negatively charged latex particles in the presence of a strong cationic polyelectrolyte at elevated ionic strengths, J. Colloid Interface Sci. 347 (2010) 202–208, http://dx.doi.org/10.1016/j.jcis.2010.03.046.
[39] J. Hierrezuelo, I. Szilagyi, A. Vaccaro, M. Borkovec, Probing nanometer-thick polyelectrolyte layers adsorbed on oppositely charged particles by dynamic light scattering, Macromolecules 43 (2010) 9108–9116, http://dx.doi.org/10.1021/ma1014462.
[40] A. Sadeghpour, E. Seyrek, I. Szilaźgyi, J. Hierrezuelo, M. Borkovec, Influence of the degree of ionization and molecular mass of weak polyelectrolytes on charging and stability behavior of oppositely charged colloidal particles, Langmuir 27 (2011) 9270–9276, http://dx.doi.org/10.1021/la201968b.